GEOV325: Glaciology

Simulating the Greenland Ice Sheet

Using a Two-Dimensional Ice Flow Model

Robert Wright

14th June 2024

University of Bergen

Contents

1. Introduction

The Greenland ice sheet (GrIS) is the second-largest body of ice in the world and covers roughly 80 % of Greenland [1]. Its average thickness is around 1.5 km, however, the ice can reach maximum depths of over 3 km.

The GrIS shrinks as climate warms, a process that can already be observed at the present day [2, Ch. 14]. While the net balance of the entire ice sheet was only slightly negative from 1960 to 1990, increased melting has occurred in subsequent years. Ice loss has generally accelerated in recent years, yet it is also superimposed by large year-to-year fluctuations. The rate of ice loss corresponded to a global sea level rise of 0.5 to 0.6 mm yr^{-1} by 2006.

The ice sheet can display non-linear responses to climate forcings due to self-perpetuating positive feedbacks [3] such as:

- Ocean warming triggers the acceleration of outlet glaciers by disintegration of their floating ice tongues (outlet glacier–acceleration feedback).

- Surface melt lowers the elevation of the ice sheet and thereby exposes it to higher temperatures (surface mass balance–elevation feedback).

Hence, uncertainties in predicting future sea level rise are predominately caused by uncer-

tainties in the climate scenarios and surface processes. Model simulations suggest that the reduction of the GrIS could contribute 5 to 33 cm to sea level by 2100, and it is projected that Greenland will very likely be ice-free within a millenium under the RCP8.5 scenario. Better quantification of these feedbacks might reveal at which point the reduction of the GrIS becomes non-reversible.

2. The Greenland ice sheet model

The GrIS is simulated using a two-dimensional ice flow model. Generally speaking, ice flow is driven by hydrostatic pressure exerting differential shear stress due to variations in glacier height. Glen's flow law, an empirical relation between strain rate and stress, allows to derive the vertically-integrated velocity

$$\overline{u} = -\frac{2}{5} A \left(\rho g \delta_x z\right)^3 h^4, \tag{1}$$

where A is the so-called flow parameter, ρ the ice density, g the gravitational acceleration, z the surface elevation, and h the ice thickness. Equation (1) can be extended to an ice flux F, which in turn, combined with the surface mass balance M (i.e., the net balance of accumulation and ablation) yields the change of ice thickness in time

$$\delta_t h = -\nabla F + M = -\nabla(\overline{u} h) + M. \tag{2}$$

2.1. Benchmarking

In order to initially verify the ice flow model, a benchmark simulation spanning 10 000 yr is performed. The spatial domain of this simulation (like all others) has a resolution of 40 km. It is run on flat bedrock, paired with an artificial surface mass balance (SMB). Inside a 10×10 grid box the SMB is positive ($M = 2\,\mathrm{m\,yr^{-1}}$), while outside this area $M = -2\,\mathrm{m\,yr^{-1}}$ is applied. Figure 1 indirectly illustrates the benchmark SMB in the upper-left subplot, since the growing ice thickness matches the area of positive SMB. On

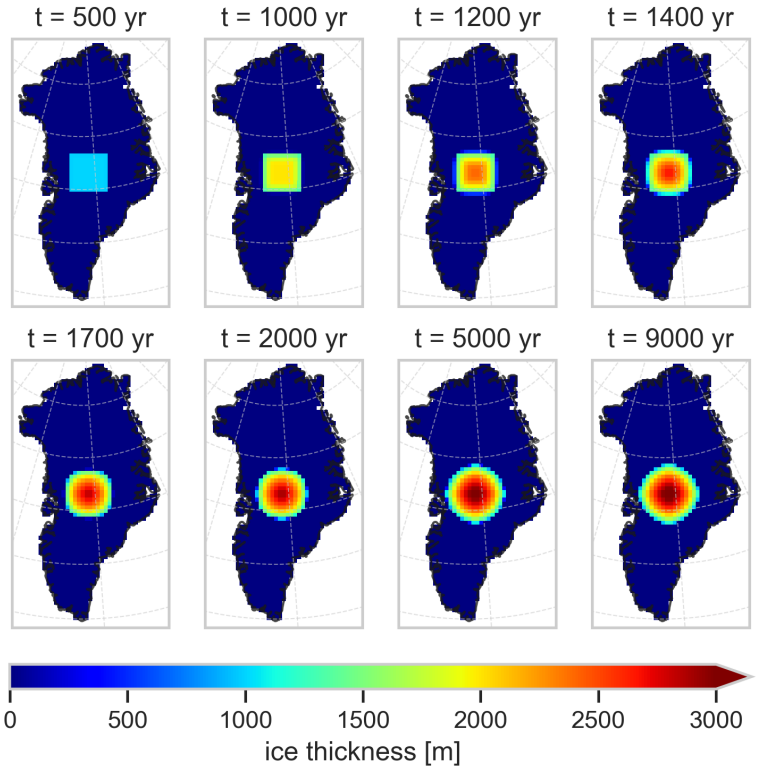

Figure 1: Map of ice thickness at time steps t during the benchmark simulation

top, we observe that the expansion of the ice ultimately reaches an equilibrium in the shape of a circle with maximum ice thickness at its centre.

The equilibrium state is characterized by a maximum ice thickness of just over 3000 m after approximately 4000 yr of simulation (fig. 2). The ice flow becomes increasingly noticeable from 1000 yr onwards, after an ice thickness of around 2000 m has been reached. From $F \propto h^5$ in eq. (2) it is to be expected that a certain height has to be reached before considerable ice flow can occur. Qualitatively, the isotropic flow and shape of the ice sheet is comparable to the results of other students and the benchmark data agrees well with what has been mentioned in the (video) lectures.

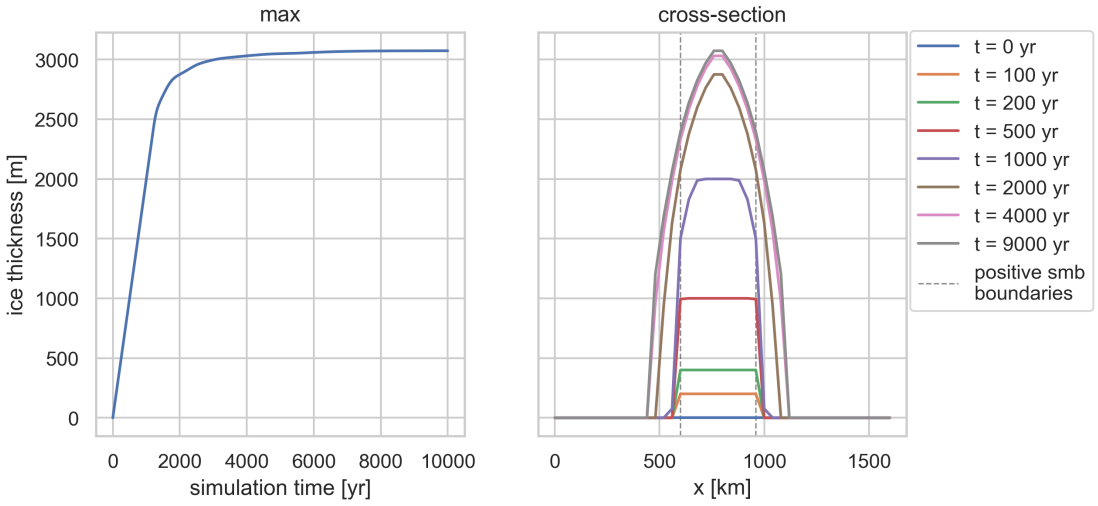

Figure 2: *Left:* Maximum ice thickness throughout simulated years. *Right:* West-east cross-section of ice thickness; the region of positive SMB is found in-between the dashed lines.

2.2. Surface mass balance

After benchmarking the simulation, the upcoming model runs feature a more realistic SMB. The annual melting M of the ice sheet is derived from an artificial temperature field T using a positive degree day approach

$$\mathrm{M} = \beta \cdot \sum_{i=\text{Jan 1}}^{\text{Dec 31}} \max\left(T_i, 0\,^\circ\mathrm{C}\right), \tag{3}$$

while the accumulation A is simplified to all precipitation P at temperatures below the freezing point

$$\mathrm{A} = \sum_{i=\text{Jan 1}}^{\text{Dec 31}} P_i, \quad \text{if } T_i < 0\,^\circ\mathrm{C}. \tag{4}$$

Combined, eqs. (3) and (4) yield the annual SMB in mm yr^{-1}. The melting factor β relates melting and accumulation (it also ensures that the SMB has the correct units) and is set to $\beta = 5\,\mathrm{mm\,d^{-1}\,^\circ C^{-1}}$ as this is within the interval of the ice and snow melting factor used by Seguinot [4].

Variable	Mechanism	Scaling factor
Temperature	Linear latitudinal gradient	North-south difference: 15 °C
	Elevation	Lapse rate: 0.65 °C/100 m
	Seasonality	Cosine function; winter-summer difference: 20 °C
	Weather	Normal distribution; standard deviation: 3.5 °C
Precipitation	Linear latitudinal gradient	North-south difference: 6 mm d^{-1}
	Euclidean distance to coastline	$[(0.1 \cdot \text{distance[\# grid points]}) + 1]^{-1}$

Table 1: Considered scaling processes to initialize temperature and precipitation fields

The artificial temperature and precipitation fields are scaled by multiple processes presented in table 1, the individual scaling factors are chosen to (roughly) match the reanalysis data in appendix B. To further confirm the choice and magnitude of the scalings, the resulting SMB displayed in fig. 3 is qualitatively compared to modelled SMB maps by Fettweis et al. [5].

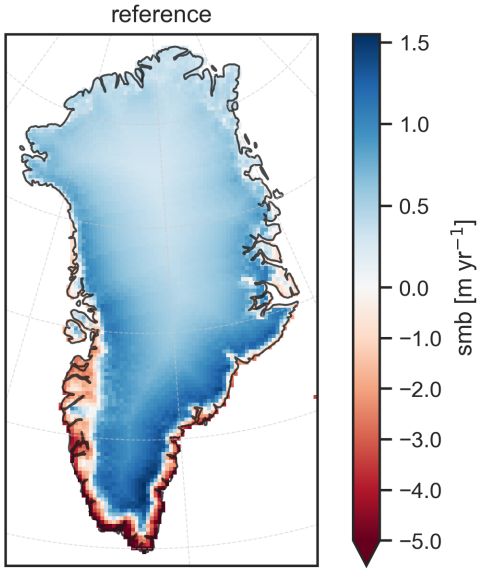

Figure 3: SMB calculated from temperature and precipitation fields based on default scaling factors introduced in table 1; please note that the colorbar uses a different scaling for positive and negative values.

3. Results

Using the benchmarked ice flow model of Greenland, in this section, the impact of varying climate scenarios on the GrIS as well as realistic projections over the next millennium are discussed.

3.1. Sensitivity to synthetic climate change

Two diverging climate scenarios are applied to the ice flow model, i.e., the climate fields used to compute the SMB are altered by varying scaling factors.

- **glacial-climate**: A glacial climate is marked by cold temperatures and low precipitation. Accordingly, the mean temperature is decreased by $\Delta\overline{T} = -13\,°\mathrm{C}$ and mean precipitation is adjusted[1] by $\Delta\overline{P} = -4\,\mathrm{mm\,d^{-1}}$ compared to the climate fields calculated from the parametrizations in table 1.

- **warm-climate**: To include a contrary scenario, this warm, moisture-rich climate is defined by $\Delta\overline{T} = 12\,°\mathrm{C}$ and $\Delta\overline{P} = 4\,\mathrm{mm\,d^{-1}}$.

Temperature influences the atmosphere's capacity to hold water vapour, changes evaporation rates and circulation patterns, hence, in this climate scenarios, both fields are altered simultaneously. The GrIS model runs for 25 000 yr, however, only the first 20 000 yr are considered in the following as this time interval is sufficient for the ice sheet to reach an equilibrium state. The simulations are initialized with present-day ice topography, and the model results based on the SMB characterized in section 2.2 act as **reference**.

Both climate scenarios ultimately reach equilibrium states of reduced GrIS volume compared to the reference model run, however, as expected, of the two scenarios, the glacial

[1] The scaling of the precipitation's latitudinal gradient is updated to be consistent with the new mean precipitation.

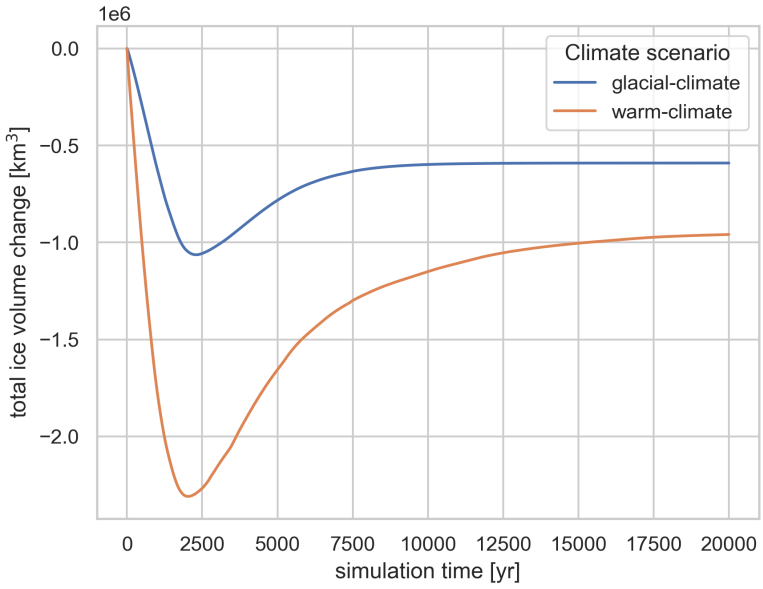

Figure 4: Change of the total GrIS ice volume in respect to the reference simulation for both climate scenarios

climate succeeds in maintaining the larger ice volume as shown in fig. 4. Here, the *continuous* difference in ice volume with respect to the reference simulation is plotted, thus, it is important to note that the reference shows a total ice volume gain of 3.32×10^6 km^3 after 5000 yr (reaching an equilibrium), which is roughly a doubling of the initial ice volume. Although one could argue that a reference should not display such an increase in ice volume, the reference's parametrization is based on published values as well as reanalysis data, thereby pointing towards limitations in trusting absolute values derived from this (rather simple) GrIS model. Interestingly, the ice volume change is characterized by a minimum in the early stage of the simulation of both climate scenarios. The glacial climate is slower in reaching an equilibrium state, hence, initially the difference in ice volume between the glacial scenario and the reference is larger. The same holds true for the warm climate, however, here melting dominates the ice volume change at first until the flow of ice compensates, and thus it takes even longer to establish an equilibrium.

To further investigate this state, fig. 5 reveals the difference in spatial distribution of ice thickness among the climate scenarios. The glacial conditions yield an ice sheet with reduced elevation, yet consistent structure, when compared to the reference, indicating that

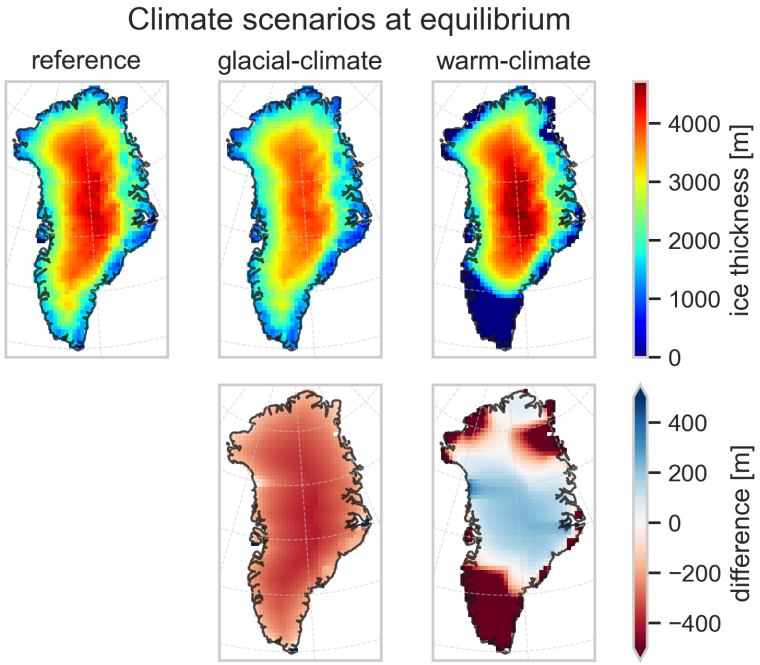

Figure 5: Ice thickness of final simulated time step; difference between climate scenario and reference below the respective scenario

the glacial climate simply cannot sustain such an elevated ice sheet due to low accumulation rates and loss of ice through transport towards the coastline (where the implemented 'calving' makes the ice disappear). The warm climate conditions show a pronounced region in the south-west where the ice sheet completely melts, on top, two areas in the north experience noticeable ice loss with respect to the reference state—on the contrary, central Greenland is characterized by an increase in ice elevation. Here, temperatures are still below freezing and thus enable accumulation, which is enhanced due to raised mean precipitation. Put together, the warm climate manages to aggregate the highest ice sheet although regions closer to the coastline experience strong ablation.

To untangle the combined effects of temperature and precipitation changes, the low numerical complexity of the GrIS allows running multiple perturbed simulations in an acceptable amount of lifetime. Following an approach by Born et al. [6], the ice flow model is either initialized with anomalous temperature fields only (ΔT) or with both anomalous temperature and precipitation fields (ΔT&ΔP). The temperature anomalies are uniformly

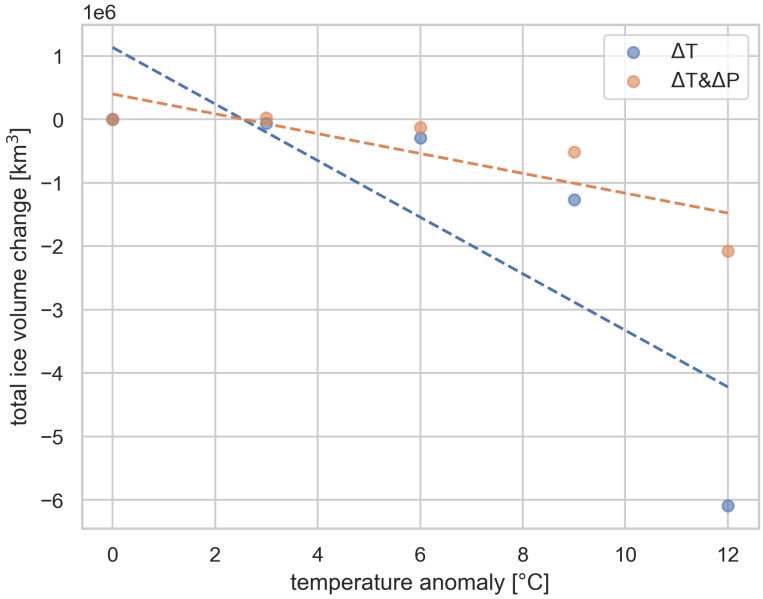

Figure 6: Change in total ice volume as a function of temperature anomaly. Either perturbation of temperature field only (blue) or perturbation of both temperature and precipitation field (orange) is applied to initialize GrIS model; dashed lines represent linear fits.

spaced from 0 to 12 °C and the precipitation anomalies from 0 to 1 mm d^{-1}, resulting in a total of eight perturbed simulations, which run until an equilibrium state is reached. The anomaly ranges are roughly extrapolated from a projection of the Norwegian Earth System Model (NorESM) for 2100 CE provided in the course. Here, an increase in mean annual temperature of $\Delta\overline{T} = 3.8\,°C$ corresponds to a positive precipitation anomaly of $\Delta\overline{P} = 0.2\,\text{mm}\,d^{-1}$.

As expected, fig. 6 shows that the total ice volume generally decreases with larger temperature anomalies, regardless of whether precipitation perturbations are applied or not. Accordingly, ΔT and ΔT&ΔP show a negative curvature, and in both cases no linear relation between temperature anomaly and ice volume change is identifiable. This non-linearity is most-likely caused by positive feedback mechanisms, such as the SMB–elevation interaction introduced in section 1.

Although the change in total ice volume does not follow a linear trend, generally speaking,

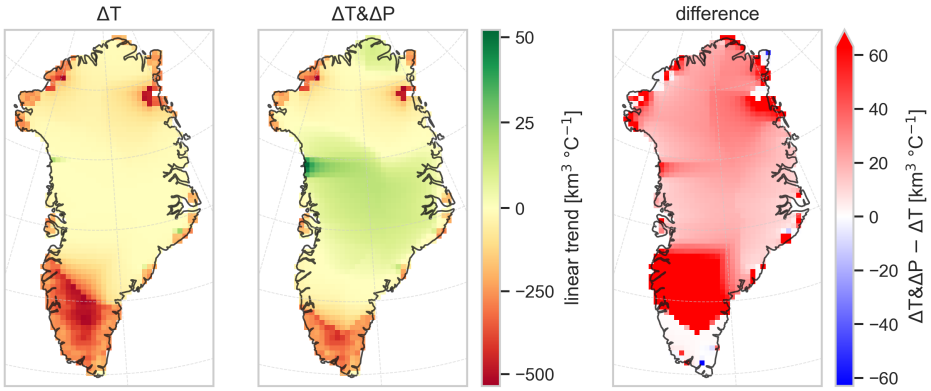

Figure 7: *Left:* Spatial distribution of the linear trend in total ice volume change as a function of temperature anomaly. Note the non-linear colour scale. *Right:* Difference of initializing simulations with anomalous temperature alone (ΔT) and with both temperature and precipitation anomalies (ΔT&ΔP).

the sign of the slope reveals whether the ice volume in- or decreases with respect to the magnitude of perturbations. Repeating the regression for each grid point of the model's spatial domain yields maps of the linear trend for ΔT and ΔT&ΔP, presented in fig. 7. If the GrIS model is perturbed with temperature anomalies only, the linear trend is predominantly negative, in particular, large negative slopes are observed in the south-west area. Including precipitation anomalies results in an increase of ice volume with higher temperatures in central Greenland. The difference of ΔT and ΔT&ΔP is overall positive, implying that more precipitation (and higher accumulation rates) can counteract increased melting in some areas. Interestingly, the pronounced difference in the south is caused by transport of ice from the elevated (growing) ice sheet in central Greenland towards the southern ablation zone, only possible in the case of ΔT&ΔP. These results also align with the previous analysis of the climate scenarios and further explain how the warm climate is able to sustain a large ice sheet in the central region.

3.2. Future of the Greenland ice sheet

The entire GrIS holds 7.4 m of sea level equivalent [7] and is sensitive to changing climate conditions. In this section, the response of the GrIS to varying climate forcings in

this millennium is simulated. Two different approaches of acquiring the temperature and precipitation fields, that in turn are used to calculate the annual SMB, are applied.

- The NorESM can be used to derive daily temperature and precipitation anomalies for 2100 CE, which, combined with the present-day climatology, yield climate fields for that particular year. To obtain a continuous forcing, the anomalies are scaled by a climate index, which is presented in appendix C.1. The scaling processes to calculate the climate fields are omitted, rather, the climate forcing is determined directly from results of complex climate models. Their output is provided as part of the course, and the corresponding climate forcing is labelled as **NorESM** in the following.

- Secondly, a rather idealized warming scenario is achieved by maintaining the SMB scalings (table 1), and adjusting the respective parameters to obtain the desired climate forcing. To establish a warming scenario analogous to the NorESM forcing, the temperature is increased by $\Delta\overline{T} = 12\,^{\circ}\mathrm{C}$ (refer to appendix C.2 for further details). In an alternative warming scenario, the temperature is raised by $\Delta\overline{T} = 4\,^{\circ}\mathrm{C}$ to receive a climate forcing that corresponds to late-21$^{\mathrm{st}}$-century conditions, following an approach by Greve and Chambers [8]. The temperature field scaling is kept constant throughout the simulation, and the respective warming scenarios are labelled as **idealized_<**$\Delta\overline{T}$**>**.

The resulting effects of the climate forcings on the GrIS during this millennium are presented in fig. 8. The simulated ice volume changes are counted positively for loss and expressed as sea-level contribution. By 3000 CE, the GrIS contributed 1.15 m (idealized_+4), 5.39 m (NorESM) or 5.96 m (idealized_+12) to global sea-level rise, depending on the warming scenario. For the more pronounced warming scenarios (NorESM and idealized_+12), this is almost equivalent to a complete ablation of the GrIS, a result confirmed by Aschwanden et al. [3]. The authors applied also an extreme warming scenario, namely, extrapolating the increasing temperature trend up until 2500 CE, after which they kept the temperature constant, and observed complete melting of the GrIS following the RCP8.5 scenario. The mass loss of the moderate climate forcing (idealized_+4) is consistent with the results of Greve and Chambers [8], who found the GrIS's sea-level contribution to amount to (1.79 ± 0.80) m SLE for RCP8.5 by 3000 CE.

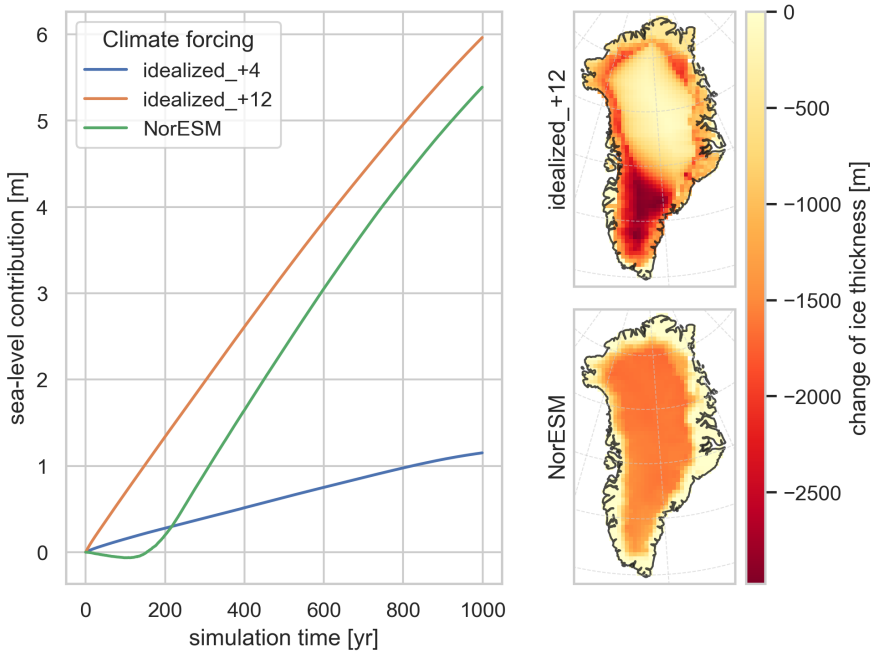

Figure 8: *Left:* Accumulated sea-level contribution until 3000 CE depending on climate forcing scenario with respect to the reference simulation (idealized_*) or the initial GrIS state (NorESM). *Right:* Difference in ice thickness at final time step of (*top*) strong idealized warming and reference, and (*bottom*) NorESM forcing scenario and present-day ice thickness.

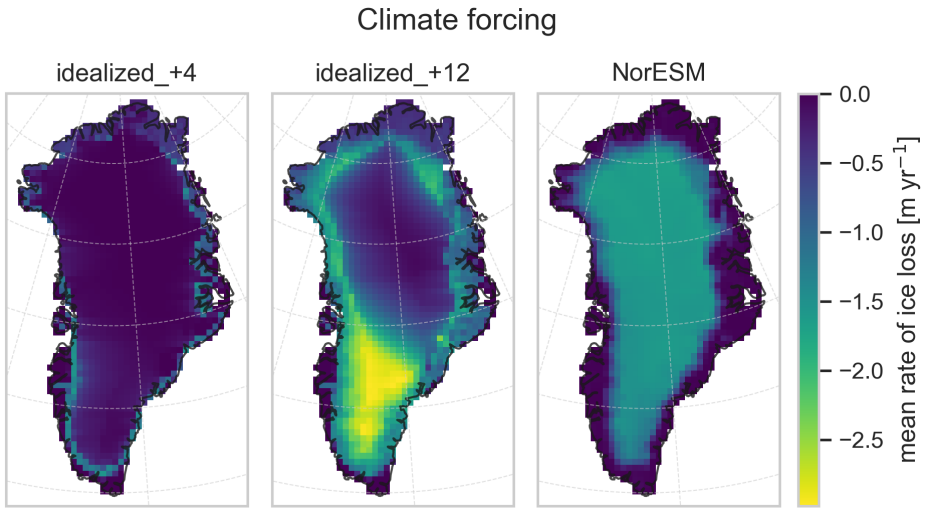

Figure 9: Spatial distribution of time-averaged gradient of ice thickness change for different climate forcing scenarios

Although the total ice loss of idealized_+12 and NorESM turns out to be roughly the same, spatially resolving the change in ice thickness (fig. 8) reveals a differing situation: While the NorESM forcing scenario leads to relatively uniformly-distributed ice loss, the idealized warming shows an area of pronounced melting in the southern part of Greenland, yet leaving the central ice sheet more or less untouched. Furthermore, if focussing on the mean rate of ice loss in fig. 9, an analogous structure is observed for the strong warming scenarios: Again, the idealized_+12 forcing displays the largest (mean) rates of ice loss in the southern region with more than $-2.5\,\mathrm{m\,yr^{-1}}$, while the NorESM forcing leads to consistent ice loss rates of around $-1.5\,\mathrm{m\,yr^{-1}}$ for most of the GrIS. Finding such similarities in the spatial distribution between the ice loss rate averaged over the entire duration of the simulation and the ice thickness change at the end of the simulation is also linked to the fact that the accumulated sea-level contribution is approximately linear in time (except for the NorESM forcing in the beginning of the simulation). The strong melting in southern Greenland might not be present in the NorESM forcing scenario as it is counteracted by high precipitation rates found in that region (see fig. 13), while the climate field scaling processes used in the idealized warming scenarios fail to reproduce such strong, localized precipitation signals. The idealized_+4 warming scenario shows moderate ice loss at the edges of the GrIS, while the centre is mainly unaffected, which matches the simulated ice thickness maps found in Greve and Chambers [8].

4. Discussion

In this study, a two-dimensional ice flow model for the GrIS was implemented from scratch. After testing and benchmarking, the model was used to analyse the GrIS's response to varying climate conditions, to separate the effects of temperature and precipitation perturbations, and to project the future of the GrIS under global warming scenarios. While the low-complexity model is time-efficient, the simplicity causes problems when initializing the model with an idealized SMB derived from present-day climate. Those simulations neither left the GrIS unchanged nor decreased the ice volume, but instead showed an increase of the ice sheet to almost twice its size. Whether the scaling processes to calculate the SMB are over-simplified, in need of improved calibration, and/or the model lacks

important internal mechanisms (e.g., bedrock sinking, basal hydrology) requires further analysis.

However, if relying on differences to a reference simulation, rather than absolute values, the model produces accurate results that also align with published estimates. It is able to reproduce the combined effect of increased temperature and precipitation resulting in an accumulation of the ice sheet in central Greenland. Generally speaking, when comparing equilibrium states of differing synthetic climate conditions, the model produces reasonable results. Additionally, if applying a realistic global warming scenario for a limited amount of simulated years, the large-scale changes are consistent with published estimates. Of course, if research requires high spatial resolution or is focussed on only a small region of Greenland, this model is not suitable, rather, it can act as a starting point of an analysis, to eventually move to more complex (and time-consuming) GrIS models.

A possible future analysis can study the impact of changes to the background climate signal, similar to what has been started with the NorESM forcing, but as the model can easily simulate thousands of years, on longer time-scales. If incorporating the Milankovitch cycles into the climate forcing, can the model produce corresponding glacial and interglacial frequencies?

References

[1] S. P. Raikar. 'Greenland Ice Sheet'. In: *Britannica* (10/06/2024). URL: https://www.britannica.com/place/Greenland-Ice-Sheet (visited on 13/06/2024).

[2] K. M. Cuffey. *The Physics of Glaciers*. Ed. by W. S. B. Paterson. 4th ed. San Diego: Elsevier Science & Technology, 2010. 1721 pp. ISBN: 9780080919126.

[3] A. Aschwanden et al. 'Contribution of the Greenland Ice Sheet to sea level over the next millennium'. In: *Science Advances* 5.6 (06/2019). ISSN: 2375-2548. DOI: 10.1126/sciadv.aav9396.

[4] J. Seguinot. 'Spatial and seasonal effects of temperature variability in a positive degree-day glacier surface mass-balance model'. In: *Journal of Glaciology* 59.218 (2013), pp. 1202–1204. ISSN: 1727-5652. DOI: 10.3189/2013jog13j081.

[5] X. Fettweis et al. 'GrSMBMIP: intercomparison of the modelled 1980–2012 surface mass balance over the Greenland Ice Sheet'. In: *The Cryosphere* 14.11 (11/2020), pp. 3935–3958. ISSN: 1994-0424. DOI: 10.5194/tc-14-3935-2020.

[6] A. Born et al. 'An efficient surface energy–mass balance model for snow and ice'. In: *The Cryosphere* 13.5 (05/2019), pp. 1529–1546. ISSN: 1994-0424. DOI: 10.5194/tc-13-1529-2019.

[7] M. Morlighem et al. 'BedMachine v3: Complete Bed Topography and Ocean Bathymetry Mapping of Greenland From Multibeam Echo Sounding Combined With Mass Conservation'. In: *Geophysical Research Letters* 44.21 (11/2017). ISSN: 1944-8007. DOI: 10.1002/2017gl074954.

[8] R. Greve and C. Chambers. 'Mass loss of the Greenland ice sheet until the year 3000 under a sustained late-21st-century climate'. In: *Journal of Glaciology* 68.269 (03/2022), pp. 618–624. ISSN: 1727-5652. DOI: 10.1017/jog.2022.9.

A. Code availability

The two-dimensional ice flow model is written in python and the entire project can be found in an online repository[2]. The ice transport equations are numerically solved in the main model part found in `2d-ice-sheet/2d_model.py`, while the SMB is externally computed and updated in the `2d-ice-sheet/surface_mass_balance.py` file. The corresponding parameters for initializing the temperature and precipitation fields are stored in the `params.py` files in the respective subdirectories.

B. SMB parametrization

In order to derive an estimate for the values of the different scaling methods in table 1, multi-year plots of the mean temperature (fig. 10) and precipitation (fig. 11) in Greenland are created based on ERA5 reanalysis data from 2010 to 2019.

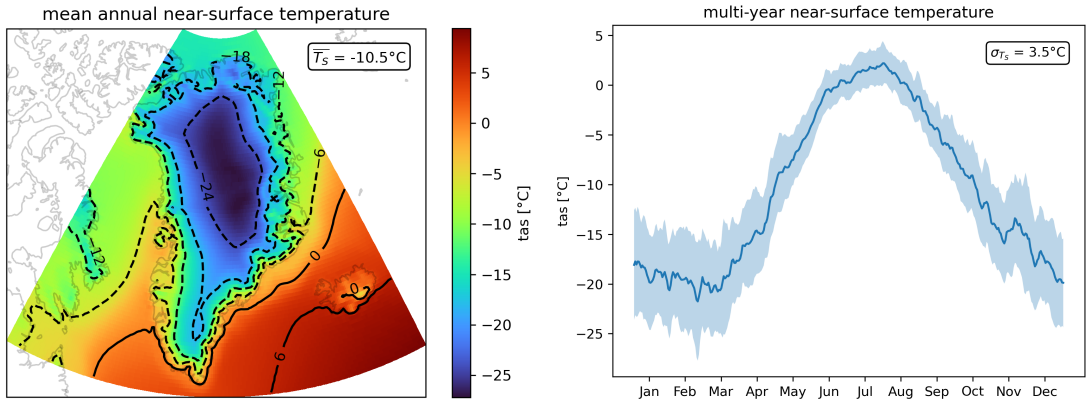

Figure 10: Spatial distribution and seasonality of temperature field

[2] `https://gitlab.met.fu-berlin.de/rw0064fu/glaciology`

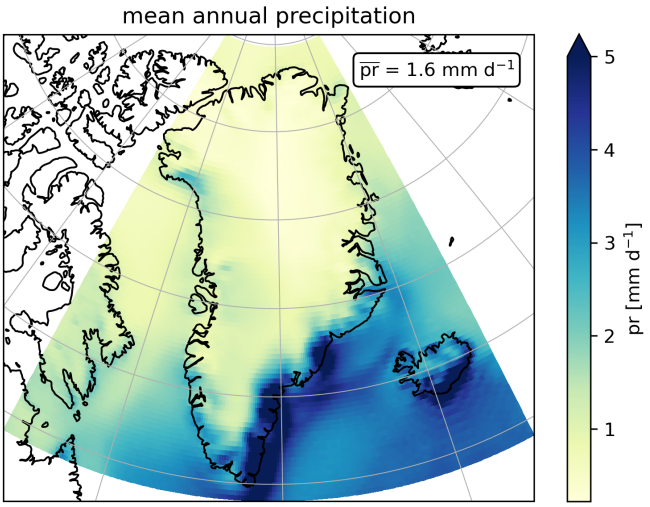

Figure 11: Precipitation field; the maximum annual precipitation is $\overline{P}_{\text{max}} = 8.84\,\text{mm}\,\text{d}^{-1}$ (not displayed by cropped colorbar)

C. Climate forcings

C.1. NorESM

The NorESM climate forcing depends on a future projection of the climatology, scaled by a climate index (fig. 12) to match the respective year of the simulation. For roughly the first 200 yr, the climate index increases, until reaching a constant value of ≈ 3 for the remaining time.

C.2. Idealized_*

The idealized_+12 forcing scenario is derived from an analysis of the climate index and the magnitude of the climate anomaly in 2100 CE, which is scaled by the climate index. Since the index peaks at ≈ 3 and the temperature anomaly is $\Delta T \approx 4\,°\text{C}$ (compare figs. 10 and 13), increasing the temperature field by $\Delta\overline{T} = 12\,°\text{C}$ yields a similar climate forcing as the NorESM case. Furthermore, Greve and Chambers [8] simulate the GrIS under

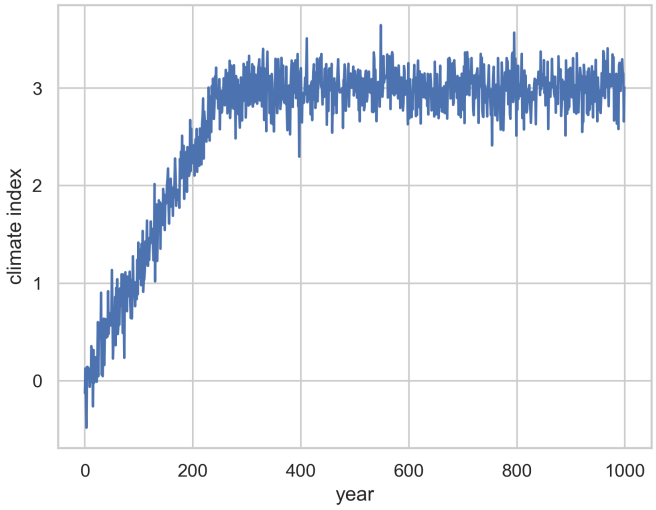

Figure 12: The climate index spans 1000 yr, and is provided as part of the glaciology course.

a sustained late-21st-century climate, hence, the temperature increase in the idealized_+4 forcing is equal to the temperature anomaly in 2100 CE. This choice is within the projected window of global temperature rise in the RCP8.5, one of the pathways used by Greve and Chambers [8].

In both scenarios, changes in precipitation are neglected ($\Delta P < 0.2\,\mathrm{mm\,d^{-1}}$) and therefore computing of precipitation fields is unaltered.

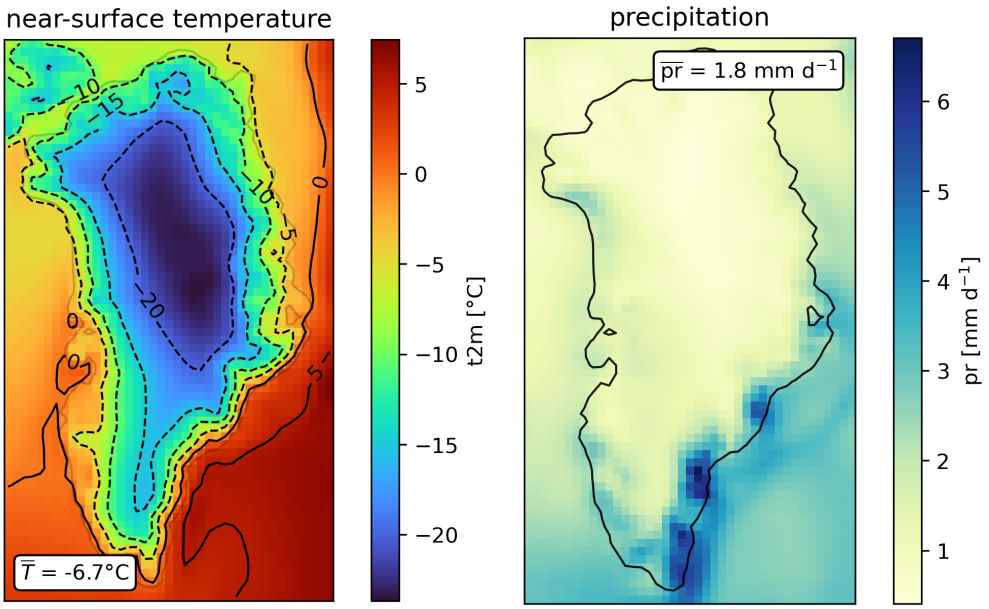

Figure 13: Annual mean near-surface temperature and precipitation for 2100 CE based on sum of projected anomalies by NorESM and present-day climatology